

Article

# Fully Coupled Multi-Scale Model for Gas Extraction from Coal Seam Stimulated by Directional Hydraulic Fracturing

Zhaolong Ge <sup>1,2,3,\*</sup>, Liang Zhang <sup>1,2,3</sup> , Juzheng Sun <sup>1</sup> and Jinhong Hu <sup>1</sup>

<sup>1</sup> State Key Laboratory of Coking Coal Exploitation and Comprehensive Utilization, Pingdingshan 467000, China; zhang\_liang@cqu.edu.cn (L.Z.); 13103651878@126.com (J.S.); hujinhong031111@163.com (J.H.)

<sup>2</sup> State Key Laboratory of Coal Mine Disaster Dynamics and Control, Chongqing University, Chongqing 400044, China

<sup>3</sup> School of Resources and safety Engineering, Chongqing University, Chongqing 400044, China

\* Correspondence: gezhaolong@cqu.edu.cn; Tel.: +86-23-6510-6640

Received: 27 September 2019; Accepted: 1 November 2019; Published: 5 November 2019



**Featured Application:** A finite element computer program, Comsol Multiphysics, was used to solve the partial differential equations in this paper.

**Abstract:** Although numerous studies have tried to explain the mechanism of directional hydraulic fracturing in a coal seam, few of them have been conducted on gas migration stimulated by directional hydraulic fracturing during coal mine methane extraction. In this study, a fully coupled multi-scale model to stimulate gas extraction from a coal seam stimulated by directional hydraulic fracturing was developed and calculated by a finite element approach. The model considers gas flow and heat transfer within the hydraulic fractures, the coal matrix, and cleat system, and it accounts for coal deformation. The model was verified using gas amount data from the NO.8 coal seam at Fengchun mine, Chongqing, Southwest China. Model simulation results show that slots and hydraulic fracture can expand the area of gas pressure drop and decrease the time needed to complete the extraction. The evolution of hydraulic fracture apertures and permeability in coal seams is greatly influenced by the effective stress and coal matrix deformation. A series of sensitivity analyses were performed to investigate the impacts of key factors on gas extraction time of completion. The study shows that hydraulic fracture aperture and the cleat permeability of coal seams play crucial roles in gas extraction from a coal seam stimulated by directional hydraulic fracturing. In addition, the reasonable arrangement of directional boreholes could improve the gas extraction efficiency. A large coal seam dip angle and high temperature help to enhance coal mine methane extraction from the coal seam.

**Keywords:** directional hydraulic fracturing; coal mine methane extraction; multi-scale model; numerical simulation

## 1. Introduction

China is one of the most severely threatened nations in terms of the risks of coal and gas outburst in underground coal mines. In recent decades, as coal mining depths have increased, the majority of low-gassy coal mines have become high-gassy and outburst-prone mines that reduce the safety and advantage of mining [1]. Coal mine methane (CMM) extraction is the most fundamental approach to eliminate the risk of coal and gas outburst. It can not only enhance coal output but also capture clean energy and reduce greenhouse gas emission [2–4]. However, particularly in southwest of China, where the coal seam permeability is lower than 0.001 mD, the flow in single-hole gas drainage from coal seams is quite low and extraction completion takes up to 2–3 years [5,6].

Hydraulic technology for increasing the permeability of coal seams, including hydraulic slotting, hydraulic fracturing, and hydraulic flushing is an effective way to increase gas drainage efficiency in low permeability coal seams. The hydraulic slotting technology uses a high-pressure waterjet to cut the coal around the borehole and form an elliptic pressure relief zone around the slot. In this area, the crustal stress is relieved and gas can be easily extracted, but the scope of its influence is small. Hydraulic fracturing has become a standard practice applied to low permeability coal seams, and it can transform the structure of coal to enhance gas extraction efficiency. It is generally believed that hydraulic fracture propagation in coal seams is subjected to the horizontal stress difference and coal seam dip angle, elastic modulus, and fracture toughness [7,8]. These primary factors could lead to disorderly propagation of hydraulic fractures and damage to the roof and floor. As a result, gas drainage from a coal seam stimulated by fracturing can be inefficient. To enlarge the slotting influence scope and resolve the issue of disorderly crack propagation in conventional hydraulic fracturing, a directional hydraulic fracturing method integrated hydraulic slotting and hydraulic fracturing is proposed [9–13], as shown in Figure 1. This method utilizes a high-pressure water jet to slot in the fracturing borehole and directional boreholes along the coal bed inclination, and then hydraulic fracturing is performed in the fracturing borehole. Through the guidance of directional boreholes, the direction of hydraulic fracture propagation follows the trend of coal seam and therefore averts damage to the roof and floor.

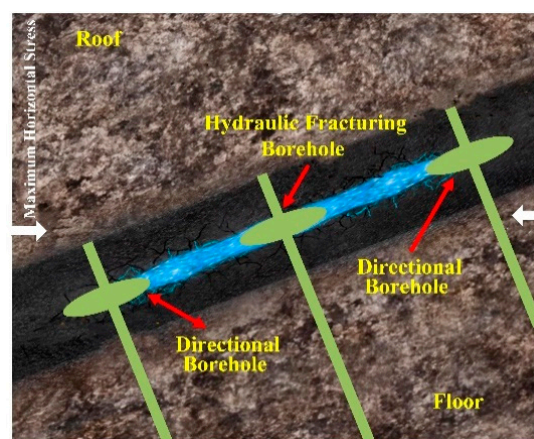


**Figure 1.** Directional hydraulic fracturing method.

In the previous study [11], when hydraulic slotting deviation angle or the horizontal stress difference is small, the hydraulic fracture can be oriented to expand along the direction of the slotting arrangement and connect fracturing borehole to slotting borehole. Coal is typical a dual-porosity reservoirs consisting of matrix and natural fractures, termed cleats [14,15]. After directional hydraulic fracturing, fractures induced by hydraulic slotting and fracturing can provide highly permeable flow channels for gas transport into boreholes. When CMM extraction process begins, the free methane within the induced fractures will flow out firstly. Then the methane in the coal matrix will desorb into these fractures and the gas pressure will decline rapidly in the coal seam. The whole process contains a series of coupling behaviors, such as coal deformation, gas flow and heat transfer within hydraulic fractures, matrix, and cleat system. Therefore, it is crucial for gas extraction from a coal seam stimulated by directional hydraulic fracturing to consider the different type of gas flow at different scales under thermo-hydro-mechanical (THM) coupling conditions (Figure 2).

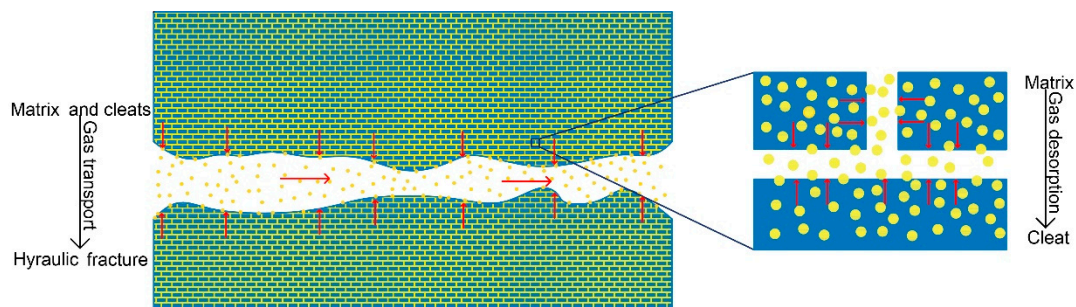


**Figure 2.** Different types of gas flow at different scales.

Previously, many models have been derived for CMM extraction or coalbed methane extraction to characterize gas migration in coal seams. Gray [16] first proposed a coal permeability related to effective stress and coal matrix shrinkage during gas drainage. Subsequently, many permeability models were developed to account for the effect of effective stress and coal matrix shrinkage [17–20]. Most of these models assumed uniaxial strain conditions, which is inconsistent with the three-dimensional in-situ stress in coal seams. To eliminate the restriction of this assumption, a sequence of new models have been introduced that account for in the in-situ stress conditions [21–24]. Based on these permeability models some scholars established coupled numerical models for coal seam methane extraction. Wu et al. [25] conducted a dual poroelastic model to quantify the interactions between  $\text{CO}_2$  and  $\text{CH}_4$  during  $\text{CO}_2$ -enhance coal seam methane recovery. Zhu et al. [26] considered thermal transport in coal to develop a THM-coupled model for investigating coal-gas interactions. Wang et al. [27] used a coupled model including equilibrium desorption model and dynamic desorption model to analyze how the non-Darcy flow influences coal seam methane extraction. Gao et al. [28] explored the gas extraction effect with slotted boreholes using a THM coupled model. A hydro-mechanical model for the modeling of coalbed methane extraction is introduced by Bertrand et al. [29]. They focused on the impact of critical parameters related to coal seams on the methane production. Through a dynamic flow model, the drainage effect after using different stimulation technologies was investigated by Szott et al. [30], where they found that the area of drainage zone after hydraulic fracturing was about 20 times larger than that after hydraulic slotting. However, none of these models is capable of investigating the multi-scale THM coupling behaviors of a coal seam after directional hydraulic fracturing. In this paper, a fully coupled multi-scale model was developed to investigate the effects of directional hydraulic fracturing on gas extraction and solved using the finite element method (FEM). This model correlates gas flow and heat transfer within the hydraulic fractures, matrix, and cleat system under deformation of the coal seam. Further, this model was validated and used to analyze the evolution of hydraulic fracture apertures and permeability in a coal seam during gas extraction. Finally, the impacts of some key factors on extraction completion time were investigated.

## 2. A Conceptual Model

Directional hydraulic fracturing is the key technique to improve coal seam permeability along a specific direction. Previous studies [9,31,32] have shown that main hydraulic fractures can be oriented in coal seams as shown in Figure 3. The computed tomography (CT) graph from [11] in Figure 3 is used here to demonstrate the phenomenon intuitively. Based on these, a model of gas extraction from coal seam after directional hydraulic fracturing was constructed in this study. In this model, a coal seam is set between two rock layers with a dip angle is  $\theta$ . Three slotting boreholes are created in the center of the coal seam. The middle slotting boreholes is a fracturing hole, and the other two slotting boreholes are directional boreholes. After hydraulic fracturing, the hydraulic fractures are presumed to directly connect the fracturing borehole and the directional boreholes, as shown in Figure 3. The maximum horizontal stress  $F_x$  is applied to the right side of the model, and the overburden stress  $F_x$  is applied to the top side. The left and base sides are roller boundaries. After directional hydraulic fracturing, the

whole coal reservoir consists of the coal matrix, cleats and hydraulic fractures. The hydraulic fractures are the major routes for gas flow induced by pressure and a modified cubic law is used to calculate the flow through them. The coal matrix and cleats have important roles in CMM extraction process. A dual porosity/dual permeability model can be applied to accurately represent the interaction of coal and methane. When negative suction pressure is applied during CMM extraction, the depletion of methane changes effective stress that influences the intrinsic permeability of the coal matrix, cleats and hydraulic fractures. Meanwhile, heat transfer modulates effective stress and gas migration in coal seam. These coupled multiphysics processes are interactive and dynamic. We converted the relationships into a number of partial differential equations and solved them with Comsol Multiphysics, a finite element method solver.

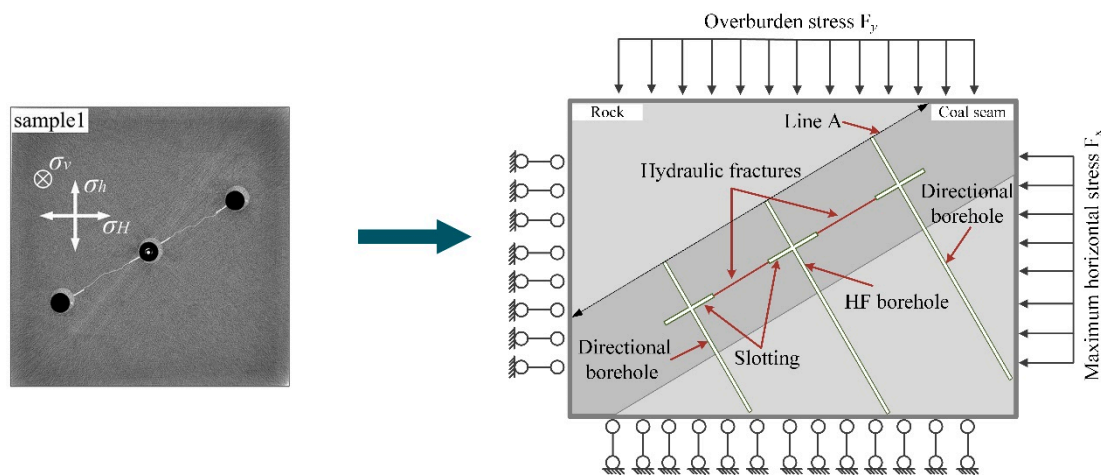


Figure 3. The geometry of the model used for numerical simulation (CT) graph adapted from [11]).

### 3. Mathematical Equations of the Conceptual Model

#### 3.1. Governing Equations of Coal Deformation

Considering thermal expansion/contraction and matrix swelling/shrinkage are isotropic, the constitutive relations for a non-isothermal dual-porosity coal seam becomes (negative in compression) [33,34]:

$$\epsilon_{ij} = \frac{1}{2G}\sigma_{ij} - \left(\frac{1}{6G} - \frac{1}{9k}\right)\sigma_{kk}\delta_{ij} + \frac{\alpha}{3K}p_m\delta_{ij} + \frac{\beta}{3K}p_f\delta_{ij} + \frac{\alpha_T}{3}T\delta_{ij} + \frac{\epsilon_s}{3}\delta_{ij} \quad (1)$$

where  $\sigma_{ij}$  is the component of total stress tensor and  $\epsilon_{ij}$  is the component of total stress tensor.  $G = D/2(1 + \nu)$ ,  $D = [1/E + 1/aK_n]^{-1}$ ,  $K = D/3(1 - 2\nu)$ ,  $\alpha = 1 - K/K_s$ ,  $\beta = 1 - K/a \cdot K_n$ ,  $K$  is the bulk modulus of coal,  $K_s$  is the bulk modulus of coal grains and  $K_n$  is the normal stiffness of individual fractures.  $E$  is the Young's modulus of coal,  $G$  is the shear modulus of coal,  $\nu$  denotes the Poisson's ratio of coal,  $\alpha$  and  $\beta$  are Biot coefficients,  $\delta_{ij}$  is the Kronecker delta,  $p$  is gas pressure, subscript  $f$  represents the cleat system,  $m$  represents the matrix system,  $T$  is temperature, and  $\alpha_T$  is thermal expansion coefficient. From Equation (1), we obtain

$$\epsilon_v = -\frac{1}{K}(\bar{\sigma} - \alpha p_m - \beta p_f) + \alpha_T T + \epsilon_s \quad (2)$$

where  $\epsilon_v = \epsilon_{11} + \epsilon_{22} + \epsilon_{33}$  is the volume strain of coal and  $\bar{\sigma} = -\sigma_{kk}/3$  is the mean stress. The sorption-induced strain  $\epsilon_s$  is generally represented by a Langmuir-type equation, which is defined as:

$$\epsilon_s = \epsilon_L \frac{p_m}{p_m + p_L} \quad (3)$$

where  $\varepsilon_L$  is the Langmuir constant representing the maximum volume strain and  $p_L$  is the Langmuir pressure constant.

The equations of stress equilibrium and the strain-displacement relationships can be expressed as:

$$\sigma_{ij,j} + f_i = 0 \tag{4}$$

$$\varepsilon_{ij} = \frac{1}{2}(u_{i,j} + u_{j,i}) \tag{5}$$

where  $f_i$  is the body force component and  $u_i$  is the displacement component. The combinations of Equations (1)–(5) yields the Navier-type equations:

$$G u_{i,jj} + \frac{G}{1-2\nu} u_{j,ii} - \beta_m p_{m,i} - \beta_f p_{f,i} - K \alpha_T T_{,i} - K \varepsilon_L \frac{P_L}{p_m + P_L} p_{m,i} + f_i = 0 \tag{6}$$

### 3.2. Governing Equations of Gas Flow in the Coal Matrix and Cleats

The gas flow in coal matrix and cleat system can be expressed with mass balance equations as:

$$\frac{\partial m}{\partial t} + \nabla \cdot (\rho_g \mathbf{q}_g) = Q_s \tag{7}$$

where  $\rho_g$  is the gas density,  $\mathbf{q}_g$  the Darcy’s velocity vector,  $Q_s$  is the gas source,  $t$  is the time, and  $m$  is the gas content, including free-phase gas and adsorbed gas. Based on the assumption that gas sorption takes places only in the matrix system, the gas content in the matrix and cleats is defined as:

$$m_m = \phi_m \rho_{gm} + \rho_n \rho_c \frac{V_L p_m}{p_m + P_L} \tag{8}$$

$$m_f = \phi_f \rho_{gf} \tag{9}$$

where  $\rho_{gm}$  and  $\rho_{gf}$  are the gas density in the matrix and cleats, respectively,  $\phi_m$  is the porosity of the matrix system,  $\phi_f$  is the porosity of the cleat system,  $\rho_n$  is the gas density under standard conditions; and  $\rho_c$  is the coal density. The density of an ideal gas is calculated by:

$$\rho_g = \frac{M_g}{RT} p \tag{10}$$

where  $M_g$  is the molecular weight of the gas and  $R$  is the universal gas constant.

The mass between the matrix and cleat system is conditioned by a smooth pressure gradient that can be written as [35]:

$$Q_s = \frac{\rho_{gm} k_m \psi}{\mu} (p_m - p_f) \tag{11}$$

where  $\mu$  is dynamic viscosity of CH<sub>4</sub>,  $k_m$  is the matrix permeability,  $\psi = 4(1/a_x^2 + 1/a_y^2)$  is the shape factor, and  $a_x$  and  $a_y$  are the matrix spacing.

Darcy’s law is used to describe gas flow in coal seams. The Darcy velocity is given by:

$$\mathbf{q}_g = -\frac{k}{\mu} \nabla p \tag{12}$$

where  $k$  is the permeability of the coal and gravity is ignored. Substituting Equations (8)–(12) into Equation (7) produces the final governing equations of gas flow in the matrix and cleat system:

$$\frac{\partial m_m}{\partial t} + \nabla \cdot \left( -\frac{k_m}{\mu} \rho_{gm} \nabla p_m \right) = -\frac{\rho_m k_m \psi}{\mu} (p_m - p_f) \tag{13}$$

$$\phi_f \frac{\partial \rho_{fg}}{\partial t} + \rho_{gf} \frac{\partial \phi_f}{\partial t} + \nabla \cdot \left( -\frac{k_f}{\mu} \rho_{gf} \nabla p_f \right) = \frac{\rho_m k_m \psi}{\mu} (p_m - p_f) \tag{14}$$

The dynamic porosity for the matrix can be expressed as [22]:

$$\phi_m = \frac{1}{1 + S} [(1 + S_0)\phi_{m0} + \alpha(S - S_0)] \tag{15}$$

where  $S = \varepsilon_v + \frac{p_m}{K_s} - \varepsilon_s - \alpha_T T$ ,  $S_0 = \varepsilon_{v0} - \frac{p_{m0}}{K_s} - \varepsilon_L \frac{p_{m0}}{p_{m0} + P_L} - \alpha_T T_0$ .

The cubic relationship of permeability and porosity is widely used for the matrix [20].

$$\frac{k}{k_0} = \left( \frac{\phi}{\phi_0} \right)^3 \tag{16}$$

where  $\phi_0$  and  $k_0$  are the initial porosity and initial permeability of the cleat system, respectively.

We substitute Equation (15) into Equation (16) to obtain:

$$k_m = k_{m0} \left( \frac{1}{1 + S} \left[ (1 + S_0) + \frac{\alpha}{\phi_{m0}} (S - S_0) \right] \right)^3 \tag{17}$$

where  $k_{m0}$  is the initial matrix permeability at the initial pressure  $p_{m0}$  and matrix porosity  $\phi_{m0}$ .

We consider the permeability anisotropy in terms of swelling/shrinkage, thermal expansion, and coal deformation for a two-dimension case with two orthogonal sets of fractures. Thus, the directional permeability  $k_{fx}$  and  $k_{fy}$  of the cleat system becomes [24]:

$$\frac{k_{fi}}{k_{f0}} = \left[ 1 + \frac{2(1 - R_m)}{\phi_{f0}} \left( \Delta \varepsilon_j - \frac{1}{3} \alpha_T \Delta T - \frac{1}{3} \Delta \varepsilon_s \right) \right]^3, i \neq j \tag{18}$$

where  $i, j = x, y$  for two-dimensional case,  $R_m = E/E_s$  is elastic modulus reduction ratio and  $\phi_{f0}$  and  $k_{f0}$  are the initial porosity and initial permeability of the cleat system, respectively.

### 3.3. Governing Equations of Gas Flow in the Hydraulic Fractures

To describe gas flow behavior of hydraulic fractures, the mass conservation equation for gas flow along the hydraulic fracture is given by:

$$\frac{\partial (w \rho_{ghf})}{\partial t} + \nabla_T \cdot (w \rho_{ghf} \mathbf{q}_{ghf}) = w Q_S \tag{19}$$

where  $w$  is the hydraulic fracture aperture,  $\rho_{ghf}$  is the gas density in the fracture and  $\mathbf{q}_{ghf}$  is gas velocity vector in the fracture. In this study, a modified cubic law was used to calculate the gas flow velocity [36]:

$$\mathbf{q}_{ghf} = -\frac{(fw)^2}{12\mu} \nabla_T p_{hf} \tag{20}$$

where  $\nabla_T p_{hf}$  is gas pressure gradient along the hydraulic fracture and  $f$  is an effective fracture conductivity parameter ranging from 0 to 1.0. When the effective stress effect is combined the swelling strain and thermal expansion effect, the hydraulic fracture aperture in soft coal seam can be expressed as:

$$w = w_0 \exp(-c_f(p_{hf0} - p_{hf})) - f \times a \left( \frac{\Delta \varepsilon_s}{3} + \frac{\alpha_T \Delta T}{3} \right) \tag{21}$$

where  $w_0$  is the initial aperture of the hydraulic fracture and  $c_f$  is the stress sensitivity coefficient for hydraulic fractures.

### 3.4. Governing Equations of Heat Transfer

According to the Fourier's law and the energy balance between the fluid and solid phases, if the convertibility between thermal and mechanical energy is ignored, the governing equation for heat transfer in a dual-porosity coal seam can be written as:

$$(pC)_M \frac{\partial T}{\partial t} + TK_g \alpha_g (\nabla \mathbf{q}_{gm} + \nabla \mathbf{q}_{gf}) + TK \alpha_T \frac{\partial \varepsilon_v}{\partial t} = \lambda_m \nabla^2 T - \rho_{gm} \mathbf{q}_{gm} C_g \nabla T - \rho_{gf} \mathbf{q}_{gf} C_g \nabla T \quad (22)$$

where  $\lambda_M = (\phi_m + \phi_f) \lambda_g + (1 - \phi_m - \phi_f) \lambda_s$ ,  $\lambda_g$  and  $\lambda_s$  are heat conductivity coefficient of coal, coal skeleton and gas, respectively,  $(pC)_M = \phi_m (\rho_{gm} C_g) + \phi_f (\rho_{gf} C_g) + (1 - \phi_m - \phi_f) (\rho_c C_s)$  is the effective heat capacity of coal,  $C_g$  and  $C_s$  are the specific heat capacity of gas and coal skeleton, respectively,  $K_g$  denotes the bulk modulus of the gas, and  $\alpha_g$  denotes the thermal expansion coefficient of the gas. Heat energy is also exchanged between the matrix and the gas in hydraulic fractures. Equation (23) is used to establish the governing equation for heat transfer in the hydraulic fracture as:

$$w \rho_{ghf} C_g \frac{\partial T_{hf}}{\partial t} + w T_{hf} K_g \alpha_g \nabla \mathbf{q}_{ghf} = w \lambda_g \nabla_T^2 T_{hf} - w \rho_{ghf} \mathbf{q}_{ghf} C_g \nabla T_{hf} - \lambda_n \frac{\partial T}{\partial n} \quad (23)$$

where  $\lambda_n \frac{\partial T}{\partial n}$  is the exchange of heat energy between the matrix and the hydraulic fracture surfaces,  $\lambda_n$  is the heat conductivity coefficient of the coal matrix in the normal direction of the fracture and  $T_{hf}$  is the gas temperature in the hydraulic fracture.

## 4. Model Validation and Results

To validate the model described in Section 2, directional hydraulic fracturing method was applied to the NO.8 coal seam at Fengchun mine, Chongqing, Southwest China (Figure 4a). The average thickness of the seam was 2 m and the coal seam dip angle was 24–28°. The coal seam permeability was less than 0.001 mD, and its roof and floor were silty sandstone that had a strong sealing capacity. The NO.8 coal seam was prone to coal and gas outbursts. Several gas accidents causing casualties and huge property losses occurred since the seam was opened. The mine operator usually waits 2–3 years to eliminate the seam outburst risk using conventional boreholes drainage method. Thus, the directional hydraulic fracturing method was utilized to improve the NO.8 coal seam permeability directionally and reduce extraction time. The BRW200/56 high-pressure pump and intelligent control device used in field experimental site are shown in Figure 4b. Field results were compared with our simulation results. Such simulation geometry used for gas extraction after directional hydraulic fracturing is shown Figure 1. The length and width of the slot was 2.1 m and 0.231 m, respectively. The directional distance was 10 m. The main parameters for the THM coupling simulation are given in Table 1. They were taken from experimental results or literatures [26,37,38].

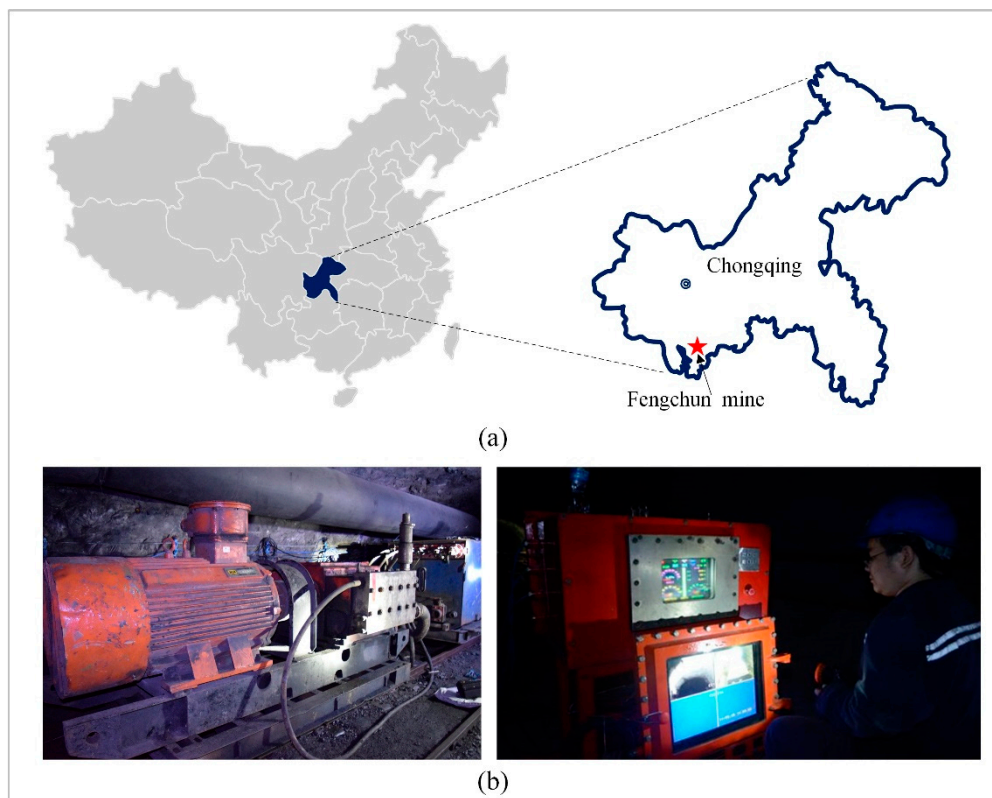


**Figure 4.** Field experimental site of directional hydraulic fracturing: (a) location of Fengchun mine in Chongqing, Southwest China and (b) the BRW200/56 high-pressure pump and intelligent control device.

**Table 1.** Main parameters for the thermo-hydro-mechanical (THM) coupling simulation.

Parameters	Value
Model dimension (m)	$30 \times 15$
Overburden stress $F_y$ (MPa)	8
Maximum horizontal stress $F_x$ (MPa)	12
Young's modulus of coal $E$ (MPa)	2100
Young's modulus of coal grains $E_s$ (MPa)	8469
Poisson's ratio of coal $\nu$	0.35
Density of coal $\rho_c$ ( $\text{kg}/\text{m}^3$ )	1380
$\text{CH}_4$ Langmuir volume constant $V_L$ ( $\text{m}^3/\text{t}$ )	34.47
$\text{CH}_4$ Langmuir pressure constant $P_L$ (MPa)	0.768
Dynamic viscosity of $\text{CH}_4$ $\mu$ ( $\text{Pa}\cdot\text{s}$ )	$1.84 \times 10^{-5}$
Temperature of boreholes (K)	293.15
Initial permeability of the fracture system $k_{f0}$ (mD)	$8.75 \times 10^{-4}$
Initial matrix permeability $k_{m0}$ (mD)	$1 \times 10^{-4}$
Initial matrix porosity $\phi_m$	0.0479
Initial hydraulic fracture aperture $w_0$ at the stress-free state (mm)	0.3
Initial Temperature of coal seam $T$ (K)	303
Maximum volume strain $\varepsilon_L$	0.004
Thermal expansion coefficient of matrix $\alpha_T$ ( $\text{K}^{-1}$ )	$2.4 \times 10^{-5}$
Specific heat capacity of coal skeleton $C_s$ ( $\text{J}/(\text{kg} \cdot \text{K})$ )	$1.25 \times 10^3$
Specific heat capacity of gas $C_g$ ( $\text{J}/(\text{kg} \cdot \text{K})$ )	$1.625 \times 10^3$
Thermal conductivity of coal skeleton $\lambda_s$ ( $\text{J}/(\text{kg} \cdot \text{K})$ )	0.2

The comparison between field data and simulation results are shown in Figure 5. It can be clearly seen that the simulations results were in good agreement with the field data for gas volume. The gas pressure distribution in the matrix at different times is presented in Figure 6. Note that pressure

around the slotting boreholes and hydraulic fractures declined most rapidly. The area of reduced gas pressure expanded gradually with increasing extraction time. In China, the government specifies that a gas pressure of 0.74 MPa is the criterion for the completion of extraction before mining operations are permitted [39]. The pre-mining extraction was equivalent to the outburst elimination time. As shown in Figure 7, the maximum residual gas pressure after 10 days was 2.49 MPa between the fracturing and the directional boreholes. This was far above the 0.74 MPa limit. As the extraction time prolonged, the residual gas pressure between boreholes decreased rapidly, and the pressure criterion of 0.74 MPa was reached after 284 days of extraction. The relative error of our simulation results was 5.96%, which confirmed that the current multi-scale THM model was applicable to a simulation of gas extraction from a coal seam stimulated by directional hydraulic fracturing.

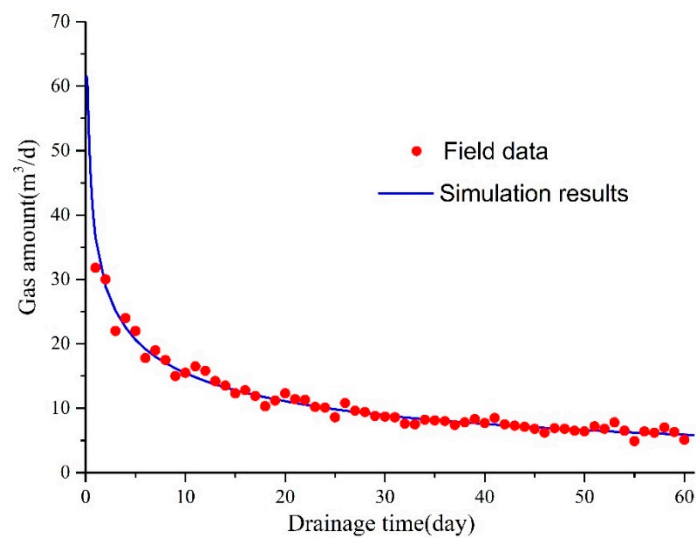


Figure 5. Comparison between field data and simulations results.

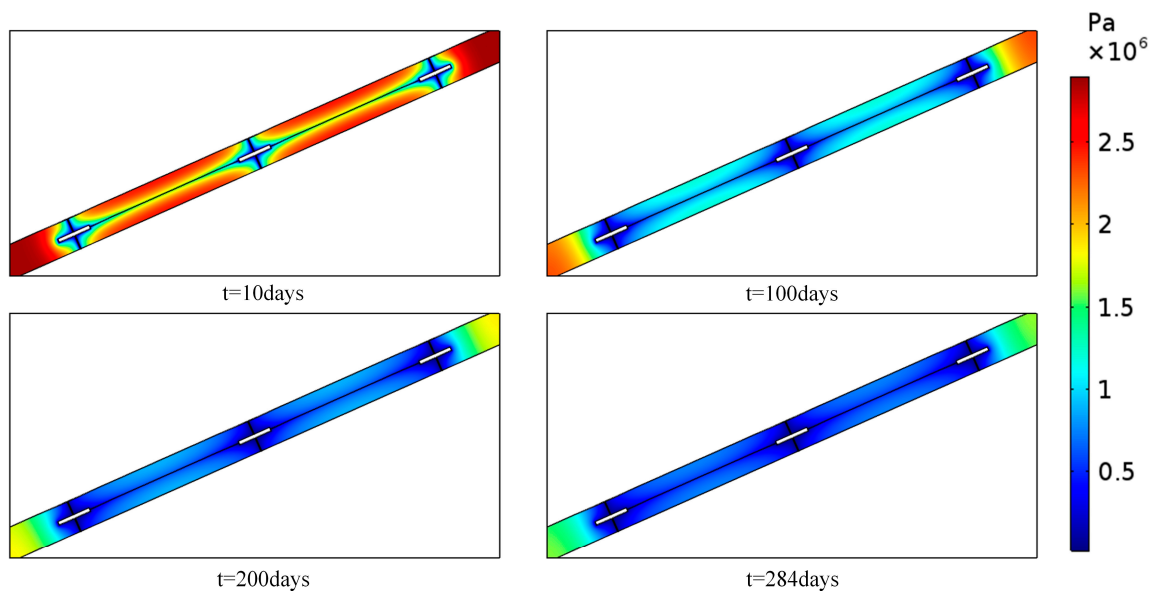


Figure 6. Gas pressure distribution of the matrix at different times.

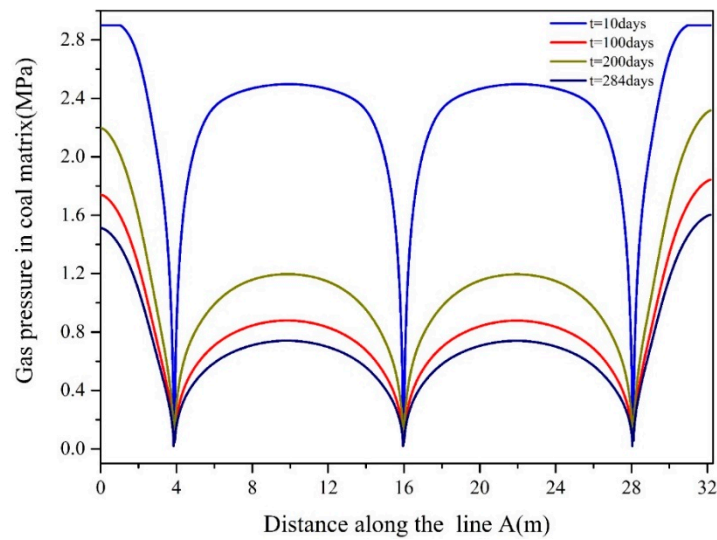


Figure 7. Gas pressure evolutions in the matrix along line A.

When the gas pressure decreased over time, the permeability of the matrix also decreased, but the cleat permeability in the x- and y-directions increased, as shown in Figure 8. The matrix and cleat permeability were both controlled by dual competing mechanism of effective stress and matrix deformation. Similar, the hydraulic fracture aperture was sensitive to the change in the effective stress. The maximum aperture of hydraulic fracture decreased from 0.229 mm at 10 days to 0.186 mm at 284 days of extraction, which indicates that the increased effective stress closed the hydraulic fracture apertures and reduced permeability and heat flux in the hydraulic fracture, as shown in Figure 9.

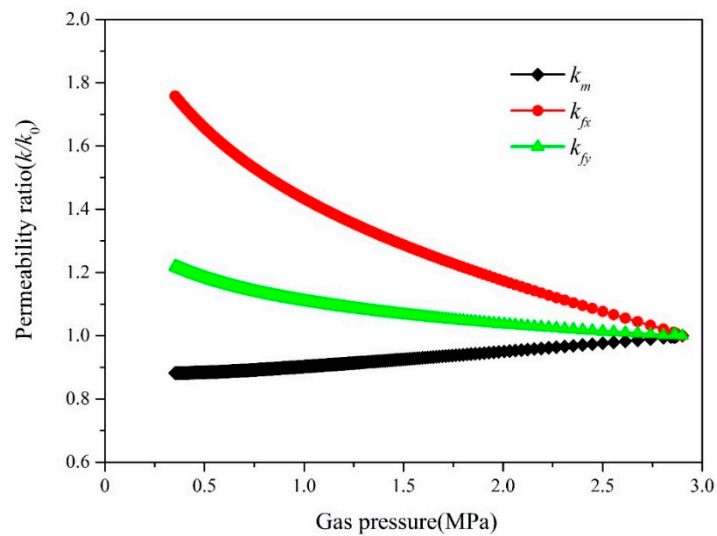
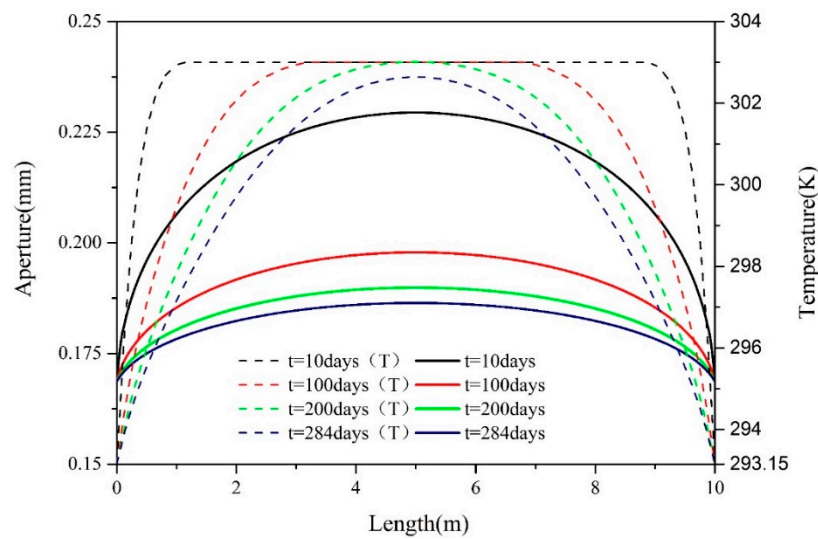


Figure 8. The evolution of the matrix and fracture permeability at a specific point  $x = 9$  m and  $y = 5.5$  m during gas drainage.



**Figure 9.** The evolution of hydraulic fracture aperture and temperature in hydraulic fracture at different times.

## 5. Discussion

In this section, we discussed how we used the base model to investigate the sensitivity of gas extraction to key factors important for the design and arrangement of fracturing boreholes and directional boreholes. The key factors included directional distance, hydraulic fracture aperture, and intrinsic permeability of the coal matrix and cleat system, coal seam dip angle and initial temperature of the coal seam.

### 5.1. Effect of Directional Distance

Different directional distance can affect the gas extraction performance. Figure 10 illustrates that the residual matrix gas pressure between boreholes increases with increased directional distance. The increased directional distance changed the time needed to complete the extraction and eliminate the outburst risk, as shown in Figure 11. When the directional distance increased from 4 m to 12 m, the extraction time increased by 1.18 times and the zone in which the gas outburst risk is eliminated was enlarged 1.42 times after 284 days of extraction. Therefore, in consideration of working faces alternation and coal seam properties, the required spacing between the fracturing and directional boreholes should be arranged reasonably to complete the extraction process effectively.

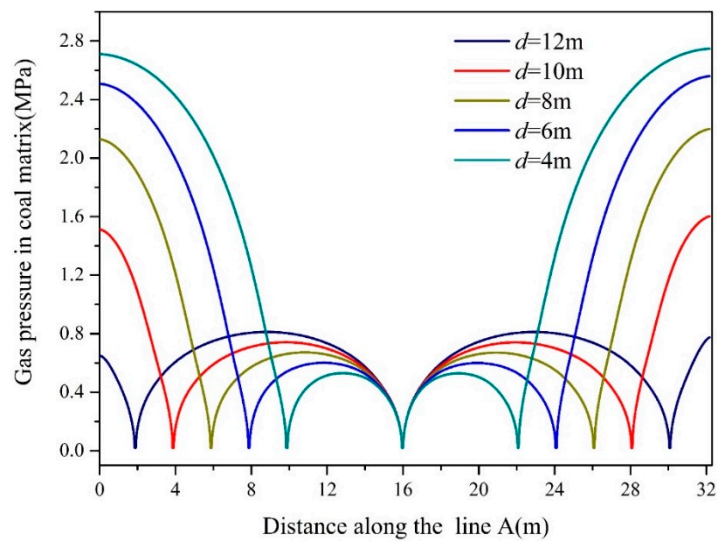


**Figure 10.** Gas pressure distribution of the matrix along line A under different directional distance after 284 days extraction.

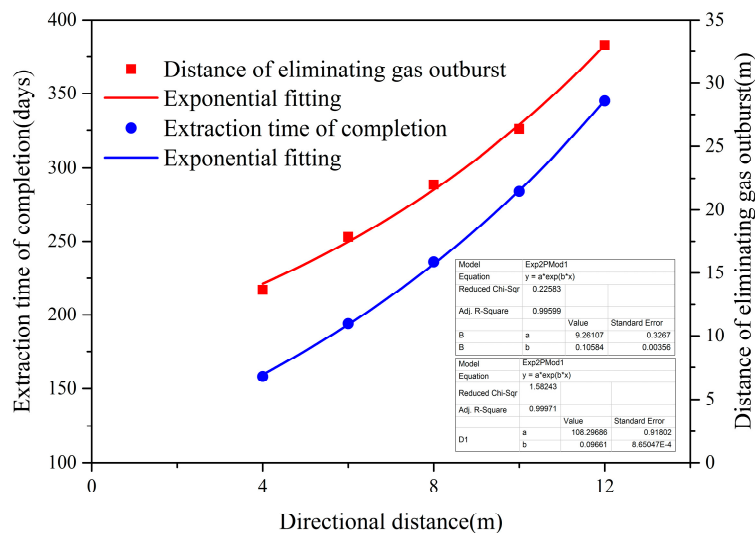


**Figure 11.** Effect of directional distance on extraction time of completion and distance of eliminating gas outburst.

### 5.2. Effect of Hydraulic Fracture Aperture

As shown in Figure 12, the extraction time of completion was highly sensitive to hydraulic fracture aperture. A larger aperture increased the gas transport through hydraulic fractures, which decreased the extraction time. When the hydraulic fracture aperture was smaller than 0.3 mm, the impact of hydraulic fracture aperture was large. The extraction time was almost 1.5 years for  $w_0 = 0.2$  mm. When the hydraulic fracture aperture increased from 0.3 mm to 0.48 mm, the extraction time decreased from 284 days to 190 days. These simulation results mean that enhancing hydraulic fracture aperture would be functional to reduce the time needed to complete the extraction.

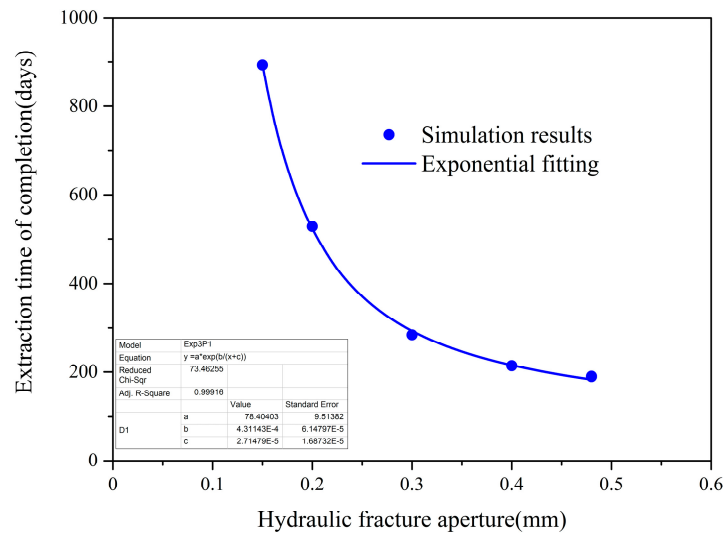


Figure 12. Effect of initial hydraulic fracture aperture on extraction time of completion.

### 5.3. Effect of the Coal Seam Dip Angle

As shown in Figure 13, the coal seam dip angle made a meaningful contribution to gas extraction time of completion. The required extraction time decreased slowly as the coal seam dip angle increase. When the directional distance changed from 0° to 28°, the extraction time was reduced from 300 days to 280 days. The reason was that different coal seam dip angle could affect the cleat permeability because of the deferent stress distribution within the seam, which increased the gas flow and reduced the extraction time.

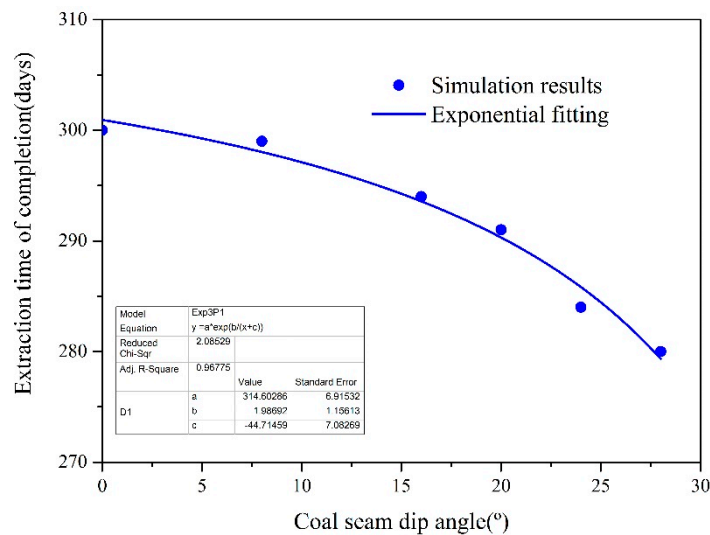


Figure 13. Effect of the coal seam dip angle on extraction time of completion.

### 5.4. Effect of the Matrix and Cleat Permeability

The matrix and cleat permeability also played a crucial role in CMM extraction. As is apparent from Figure 14, the extraction time of completion was shorter for the matrix and cleat system with higher permeability. When  $k_{m0}$  or  $k_{f0}$  increased from  $0.1 \times 10^{-3}$  mD to  $0.9 \times 10^{-3}$  mD, the extraction time of completion decreased by 21.8% and 69.5%, respectively. The extraction time of completion was more sensitive to the cleat permeability than to the matrix permeability. Since high permeability of the cleat system improved gas extraction efficiency, many fracture treatment methods were adopted to create bigger fractures within the coal seam and enhance its permeability.

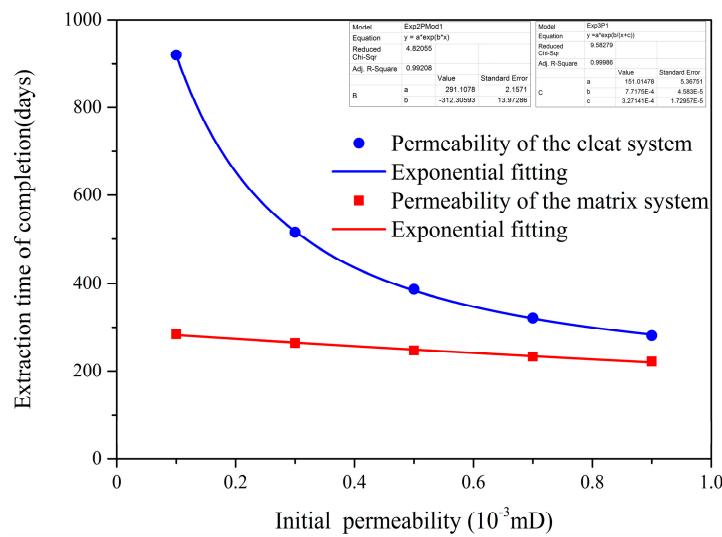


Figure 14. Effect of the matrix and fracture permeability on extraction time of completion.

### 5.5. Effect of the Initial Temperature

Temperature was also a key parameter for gas extraction that cannot be neglected. Figure 15 illustrates that the effect of the initial temperature on extraction completion time. The figures shows that increasing the initial temperature of the coal seam could decrease the time needed to complete extraction, by 3.8% when the initial temperature was increased from 298 K to 318 K. The data demonstrated that higher temperatures were conducive to faster gas extraction from a coal seam. If gas was extracted from a higher temperature coal seam, more methane desorption and temperature reduction would cause the coal matrix to shrink and increased the cleat permeability. Methane would move into boreholes more easily.

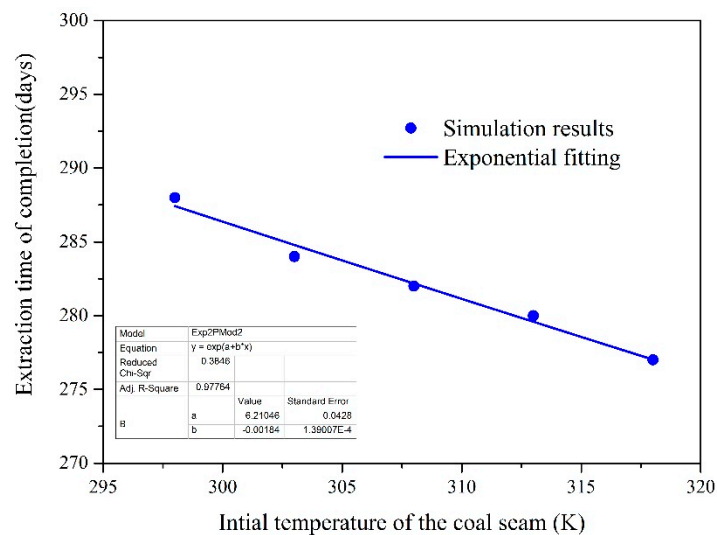


Figure 15. Effect of the initial temperature on extraction time of completion.

## 6. Conclusions

In this study, a fully coupled multi-scale model for gas extraction in a coal seam stimulated by directional hydraulic fracturing was developed and verified by gas amount data from an actual coal mine. Based on a modified cubic law and conventional dual-porosity/dual-permeability model, the model couples gas flow and heat transfer within the hydraulic fractures, the matrix and cleat system as the coal deforms while gas was extracted. Using the established model, the evolution of hydraulic

fracture aperture and permeability in a coal seam was analyzed and the sensitivity of gas extraction to key factors was investigated. The main conclusions are as follows:

(1) The evolution of hydraulic fracture aperture and permeability in a coal seam were closely related to effective stress and coal matrix deformation. They were key factors to limit the speed of gas extraction from a coal seam. Enhancing hydraulic fracture aperture and the cleat permeability of a coal seam resulted in a significant decrease in the time needed for gas extraction.

(2) The relationship between the extraction time of completion and directional distance was exponential. Larger directional distance increased the extraction time of completion and enlarged the zone with reduced outburst risk. The required spacing between the fracturing borehole and the directional borehole should be arranged reasonably according to working faces alternation and coal seam properties.

(3) The coal seam dip angle and temperature had a measurable effect on gas extraction. The extraction time of completion followed an exponential relationship with both of them. A large coal seam dip angle and high temperature helped to enhance gas extraction from a coal seam.

**Author Contributions:** Z.G. and L.Z. contributed to conceiving and developing this fully coupled model, analyzing the results of simulation, and writing the paper. J.S. and J.H. performed the verification experiment.

**Funding:** This study was jointly Funded by Open Research Fund of State Key Laboratory of Coking Coal Exploitation and Comprehensive Utilization, China Pingmei Shenma Group (Grant NO. 41040220171106-1) and the National Natural Science Foundation of China (Grant No. 51625401, NO. 51774055 and NO. 51804055).

**Acknowledgments:** The authors acknowledge the Fengchun mine for providing access to the field test site.

**Conflicts of Interest:** The authors declare no conflict of interest.

## References

- Xia, T.; Zhou, F.; Wang, X.; Zhang, Y.; Li, Y.; Kang, J.; Liu, J. Controlling factors of symbiotic disaster between coal gas and spontaneous combustion in longwall mining gobs. *Fuel* **2016**, *182*, 886–896. [[CrossRef](#)]
- Karacan, C.Ö.; Ruiz, F.A.; Cotè, M.; Phipps, S. Coal mine methane: A review of capture and utilization practices with benefits to mining safety and to greenhouse gas reduction. *Int. J. Coal Geol.* **2011**, *86*, 121–156. [[CrossRef](#)]
- Zheng, C.; Chen, Z.; Kizil, M.; Aminossadati, S.; Zou, Q.; Gao, P. Characterisation of mechanics and flow fields around in-seam methane gas drainage borehole for preventing ventilation air leakage: A case study. *Int. J. Coal Geol.* **2016**, *162*, 123–138. [[CrossRef](#)]
- Dong, J.; Cheng, Y.; Jin, K.; Zhang, H.; Liu, Q.; Jiang, J.; Hu, B. Effects of diffusion and suction negative pressure on coalbed methane extraction and a new measure to increase the methane utilization rate. *Fuel* **2017**, *197*, 70–81. [[CrossRef](#)]
- Lu, Y.; Liu, Y.; Li, X.; Kang, Y. A new method of drilling long boreholes in low permeability coal by improving its permeability. *Int. J. Coal Geol.* **2010**, *84*, 94–102. [[CrossRef](#)]
- Lu, T.; Yu, H.; Zhou, T.; Mao, J.; Guo, B. Improvement of methane drainage in high gassy coal seam using waterjet technique. *Int. J. Coal Geol.* **2009**, *79*, 40–48. [[CrossRef](#)]
- Lu, Y.; Cheng, Y.; Ge, Z.; Cheng, L.; Zuo, S.; Zhong, J. Determination of Fracture Initiation Locations during Cross-Measure Drilling for Hydraulic Fracturing of Coal Seams. *Energies* **2016**, *9*, 358. [[CrossRef](#)]
- Jiang, T.; Zhang, J.; Wu, H. Experimental and numerical study on hydraulic fracture propagation in coalbed methane reservoir. *J. Nat. Gas Sci. Eng.* **2016**, *35*, 455–467. [[CrossRef](#)]
- Yan, F.; Lin, B.; Zhu, C.; Shen, C.; Zou, Q.; Guo, C.; Liu, T. A novel ECBM extraction technology based on the integration of hydraulic slotting and hydraulic fracturing. *J. Nat. Gas Sci. Eng.* **2015**, *22*, 571–579. [[CrossRef](#)]
- Mao, R.; Feng, Z.; Liu, Z.; Zhao, Y. Laboratory hydraulic fracturing test on large-scale pre-cracked granite specimens. *J. Nat. Gas Sci. Eng.* **2017**, *44*, 278–286. [[CrossRef](#)]
- Cheng, Y.; Lu, Y.; Ge, Z.; Cheng, L.; Zheng, J.; Zhang, W. Experimental study on crack propagation control and mechanism analysis of directional hydraulic fracturing. *Fuel* **2018**, *218*, 316–324. [[CrossRef](#)]
- Lu, Y.; Ge, Z.; Yang, F.; Xia, B.; Tang, J. Progress on the hydraulic measures for grid slotting and fracking to enhance coal seam permeability. *Int. J. Min. Sci. Technol.* **2017**, *27*, 867–871. [[CrossRef](#)]

13. Cheng, L.; Ge, Z.; Xia, B.; Li, Q.; Tang, J.; Cheng, Y.; Zuo, S. Research on Hydraulic Technology for Seam Permeability Enhancement in Underground Coal Mines in China. *Energies* **2018**, *11*, 427. [[CrossRef](#)]
14. Warren, J.E. The behavior of naturally fractured reservoirs. *Soc. Pet. Eng. J.* **1963**, *3*, 245–255. [[CrossRef](#)]
15. Laubach, S.E.; Marrett, R.A.; Olson, J.E.; Scott, A.R. Characteristics and origins of coal cleat: A review. *Int. J. Coal Geol.* **1998**, *35*, 175–207. [[CrossRef](#)]
16. Gray, I. Reservoir engineering in coal seams. *SPE Reserv. Eng.* **1987**, *2*, 28–34. [[CrossRef](#)]
17. Seidle, J.; Huitt, L. Experimental Measurement of Coal Matrix Shrinkage Due to Gas Desorption and Implications for Cleat Permeability Increases. In Proceedings of the International Meeting on Petroleum Engineering, Beijing, China, 14–17 November 1995.
18. Palmer, I.; Mansoori, J. How Permeability Depends on Stress and Pore Pressure in Coalbeds: A New Model. *SPE Reserv. Eval. Eng.* **1996**, *1*, 539–544. [[CrossRef](#)]
19. Shi, J.Q.; Durucan, S. Drawdown Induced Changes in Permeability of Coalbeds: A New Interpretation of the Reservoir Response to Primary Recovery. *Transp. Porous Media* **2004**, *56*, 1–16. [[CrossRef](#)]
20. Cui, X.; Bustin, R.M. Volumetric strain associated with methane desorption and its impact on coalbed gas production from deep coal seams. *AAPG Bull.* **2005**, *89*, 1181–1202. [[CrossRef](#)]
21. Robertson, E.P.; Christiansen, R.L. A Permeability Model for Coal and Other Fractured, Sorptive-Elastic Media. *SPE J.* **2006**, *13*, 314–324. [[CrossRef](#)]
22. Zhang, H.; Liu, J.; Elsworth, D. How sorption-induced matrix deformation affects gas flow in coal seams: A new FE model. *Int. J. Rock Mech. Min. Sci.* **2008**, *45*, 1226–1236. [[CrossRef](#)]
23. Connell, L.D.; Lu, M.; Pan, Z. An analytical coal permeability model for tri-axial strain and stress conditions. *Int. J. Coal Geol.* **2010**, *84*, 103–114. [[CrossRef](#)]
24. Liu, J.; Chen, Z.; Elsworth, D.; Miao, X.; Mao, X. Linking gas-sorption induced changes in coal permeability to directional strains through a modulus reduction ratio. *Int. J. Coal Geol.* **2010**, *83*, 21–30. [[CrossRef](#)]
25. Wu, Y.; Liu, J.; Chen, Z.; Elsworth, D.; Pone, D. A dual poroelastic model for CO<sub>2</sub>-enhanced coalbed methane recovery. *Int. J. Coal Geol.* **2011**, *86*, 177–189. [[CrossRef](#)]
26. Zhu, W.C.; Wei, C.H.; Liu, J.; Qu, H.Y.; Elsworth, D. A model of coal–gas interaction under variable temperatures. *Int. J. Coal Geol.* **2011**, *86*, 213–221. [[CrossRef](#)]
27. Wang, J.G.; Kabir, A.; Liu, J.; Chen, Z. Effects of non-Darcy flow on the performance of coal seam gas wells. *Int. J. Coal Geol.* **2012**, *93*, 62–74. [[CrossRef](#)]
28. Gao, F.; Xue, Y.; Gao, Y.; Zhang, Z.; Teng, T.; Liang, X. Fully coupled thermo-hydro-mechanical model for extraction of coal seam gas with slotted boreholes. *J. Nat. Gas Sci. Eng.* **2016**, *31*, 226–235. [[CrossRef](#)]
29. Bertrand, F.; Cerfontaine, B.; Collin, F. A fully coupled hydro-mechanical model for the modeling of coalbed methane recovery. *J. Nat. Gas Sci. Eng.* **2017**, *46*, 307–325. [[CrossRef](#)]
30. Szott, W.; Słota-Valim, M.; Gołabek, A.; Łętkowski, P. Numerical studies of improved methane drainage technologies by stimulating coal seams in multi-seam mining layouts. *Int. J. Rock Mech. Min. Sci.* **2018**, *108*, 157–168. [[CrossRef](#)]
31. Liu, Y.; Xia, B.; Liu, X. A novel method of orienting hydraulic fractures in coal mines and its mechanism of intensified conduction. *J. Nat. Gas Sci. Eng.* **2015**, *27*, 190–199. [[CrossRef](#)]
32. Wang, Y.F.; Li, Y.Z. Technology and application of directional hydraulic penetration permeability improvement by guided groove. *J. China Coal Soc.* **2012**, *37*, 1326–1331.
33. Wu, Y.; Liu, J.; Elsworth, D.; Chen, Z.; Connell, L.; Pan, Z. Dual poroelastic response of a coal seam to CO<sub>2</sub> injection. *Int. J. Greenh. Gas Control* **2010**, *4*, 668–678. [[CrossRef](#)]
34. Liu, J.; Chen, Z.; Elsworth, D.; Qu, H.; Chen, D. Interactions of multiple processes during CBM extraction: A critical review. *Int. J. Coal Geol.* **2011**, *87*, 175–189. [[CrossRef](#)]
35. Lim, K.T.; Aziz, K. Matrix-fracture transfer shape factors for dual-porosity simulators. *J. Pet. Sci. Eng.* **1995**, *13*, 169–178. [[CrossRef](#)]
36. Witherspoon, P.A.; Wang, J.S.Y.; Iwai, K.; Gale, J.E. Validity of Cubic Law for fluid flow in a deformable rock fracture. *Water Resour. Res.* **1980**, *16*, 1016–1024. [[CrossRef](#)]
37. Ge, Z.; Mei, X.; Jia, Y.; Lu, Y.; Xia, B. Influence radius of slotted borehole drainage by high pressure water jet. *J. Ming Saf. Eng.* **2014**, *31*, 657–664.

38. Xia, T.; Zhou, F.; Liu, J.; Hu, S.; Liu, Y. A fully coupled coal deformation and compositional flow model for the control of the pre-mining coal seam gas extraction. *Int. J. Rock Mech. Min. Sci.* **2014**, *72*, 138–148. [[CrossRef](#)]
39. China State Administration of Work Safety. *Specification of Coal and Gas Outburst Prevention*; China Coal Industry Press: Beijing, China, 2009.



© 2019 by the authors. Licensee MDPI, Basel, Switzerland. This article is an open access article distributed under the terms and conditions of the Creative Commons Attribution (CC BY) license (<http://creativecommons.org/licenses/by/4.0/>).